

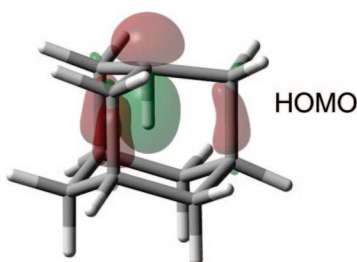
## *In*-Adamantane, a Small Inside-Out Molecule

Karl K. Irikura\*

Physical and Chemical Properties Division, National Institute of Standards and Technology,  
Gaithersburg, Maryland 20899-8380

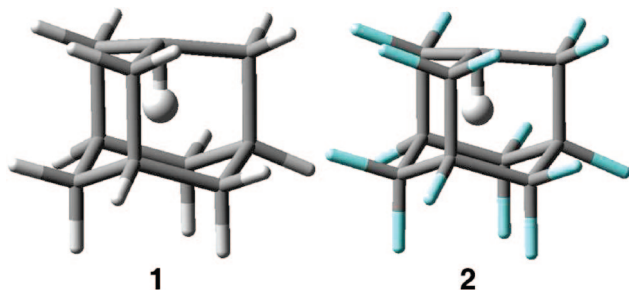
karl.irikura@nist.gov

Received August 12, 2008



The hydrocarbon *in*-adamantane (**1**), a high-energy adamantane isomer in which one methine hydrogen atom is inside the cage, is predicted by ab initio calculations to be isolable at dry ice temperature. It has 440 kJ/mol of hydrogenic strain but appears to be stable against dimerization, moisture, and air. The inverted CH bond is compressed, and the IR and NMR spectra are unusual. The symmetrical pentadecafluoro derivative (**2**) has an estimated half-life of 100 years at room temperature.

Highly strained molecules are interesting for many reasons. They pose synthetic challenges, improve our understanding of the limits of chemical bonding, display appealing and exotic structures, and have high energy densities appropriate for advanced explosives and propellants.<sup>1–3</sup> Strain in organic molecules is usually found in the carbon or heteroatom framework of a molecule, but strain can arise even from the displacement of a hydrogen atom. Described below are predictions of small, stable, hydrogen-strained molecules.



Calculations<sup>4–6</sup> using both hybrid density functional theory (B3LYP) and second-order perturbation theory (MP2) indicate that compounds **1** (*in*-C<sub>10</sub>H<sub>16</sub>) and **2** (*in*-C<sub>10</sub>F<sub>15</sub>H) are minima

on their respective potential energy surfaces; that is, all vibrational frequencies are real-valued. This means that they are isolable in principle. However, kinetic stability is important for deciding whether they are reasonable synthetic targets. Transition structures connecting inverted and conventional isomers, denoted<sup>7</sup> *in* and *out*, have therefore been determined. The reaction coordinate involves the inverted H-atom rotating through a broken  $\alpha$ -CC bond. Zero-temperature energies, including higher-level coupled-cluster results, are summarized

(3) Roy, G. D. *J. Propuls. Power* **2000**, *16*, 546–551.

(4) Frisch, M. J.; Trucks, G. W.; Schlegel, H. B.; Scuseria, G. E.; Robb, M. A.; Cheeseman, J. R.; Montgomery, J. A., Jr.; Vreven, T.; Kudin, K. N.; Burant, J. C.; Millam, J. M.; Iyengar, S. S.; Tomasi, J.; Barone, V.; Mennucci, B.; Cossi, M.; Scalmani, G.; Rega, N.; Petersson, G. A.; Nakatsuji, H.; Hada, M.; Ehara, M.; Toyota, K.; Fukuda, R.; Hasegawa, J.; Ishida, M.; Nakajima, T.; Honda, Y.; Kitao, O.; Nakai, H.; Klene, M.; Li, X.; Knox, J. E.; Hratchian, H. P.; Cross, J. B.; Adamo, C.; Jaramillo, J.; Gomperts, R.; Stratmann, R. E.; Yazyev, O.; Austin, A. J.; Cammi, R.; Pomelli, C.; Ochterski, J. W.; Ayala, P. Y.; Morokuma, K.; Voth, G. A.; Salvador, P.; Dannenberg, J. J.; Zakrzewski, V. G.; Dapprich, S.; Daniels, A. D.; Strain, M. C.; Farkas, O.; Malick, D. K.; Rabuck, A. D.; Raghavachari, K.; Foresman, J. B.; Ortiz, J. V.; Cui, Q.; Baboul, A. G.; Clifford, S.; Cioslowski, J.; Stefanov, B. B.; Liu, G.; Liashenko, A.; Piskorz, P.; Komaromi, I.; Martin, R. L.; Fox, D. J.; Keith, T.; Al-Laham, M. A.; Peng, C. Y.; Nanayakkara, A.; Challacombe, M.; Gill, P. M. W.; Johnson, B.; Chen, W.; Wong, M. W.; Gonzalez, C.; Pople, J. A. *Gaussian 03*; Gaussian, Inc.: Pittsburgh, PA, 2003.

(5) Werner, H.-J.; Knowles, P. J.; Lindh, R.; Manby, F. R.; Schütz, M.; Celani, P.; Korona, T.; Rauhut, G.; Amos, R. D.; Bernhardsson, A.; Berning, A.; Cooper, D. L.; Deegan, M. J. O.; Dobbyn, A. J.; Eckert, F.; Hampel, C.; Hetzer, G.; Lloyd, A. W.; McNicholas, S. J.; Meyer, W.; Mura, M. E.; Nicklass, A.; Palmieri, P.; Pitzer, R.; Schumann, U.; Stoll, H.; Stone, A. J.; Tarroni, R.; Thorsteinsson, T. *Molpro (vers. 2006.1)*; University College Cardiff Consultants Ltd.: Cardiff, UK, 2006.

(1) Hopf, H. *Classics in Hydrocarbon Chemistry*; Wiley-VCH: Weinheim, 2000.

(2) Eaton, P. E.; Zhang, M. X.; Gilardi, R.; Gelber, N.; Iyer, S.; Surapaneni, R. *Propellants Explosives Pyrotechnics* **2002**, *27*, 1–6.

**TABLE 1.** Reaction Energies and Barriers (kJ mol<sup>-1</sup> at *T* = 0) for Isomerization of **1** and **2** to Their Conventional *Out* Isomers

calculation	$\Delta H(1)$	$\Delta H^\ddagger(1)$	$\Delta H(2)$	$\Delta H^\ddagger(2)$
MP2	-487	81	-476	135
CCSD(T) <sup>a</sup>	-486	76	-477	129
CCSD(T)-ext <sup>b</sup>	-440	71	-421	133

<sup>a</sup> CCSD(T)/6-31G(d)//MP2/6-31G(d). <sup>b</sup> Estimated CCSD(T)/aug-cc-pVTZ.

in Table 1. The barriers in the final row of Table 1 correspond to half-lives of 30 ms and 100 years for **1** and **2**, respectively, at *T* = 298 K. At dry ice temperature (*T* = 195 K), the predicted half-life for **1** is 2 days. Large singlet and triplet vertical electronic excitation energies of 5.2 and 5.1 eV for **1** and 8.1 and 7.8 eV for **2** are additional indicators of unimolecular stability. The computed half-life of **1** when deuteriated in the *in* position (1-*d*-1-*in*-C<sub>10</sub>H<sub>15</sub>D) is 100 ms at room temperature and 2 weeks at dry ice temperature. The increase in stability upon deuteration is due to zero-point energy effects, which are accentuated by the high vibrational frequencies (see below).

The higher isomerization barrier for **2** may be ascribed, in part, to stronger C–C bonding; the C–C bond dissociation enthalpy in C<sub>2</sub>F<sub>6</sub> is stronger than in C<sub>2</sub>H<sub>6</sub> by 32 kJ mol<sup>-1</sup> (34 kJ mol<sup>-1</sup> from calculations like those in Table 1).<sup>8</sup>

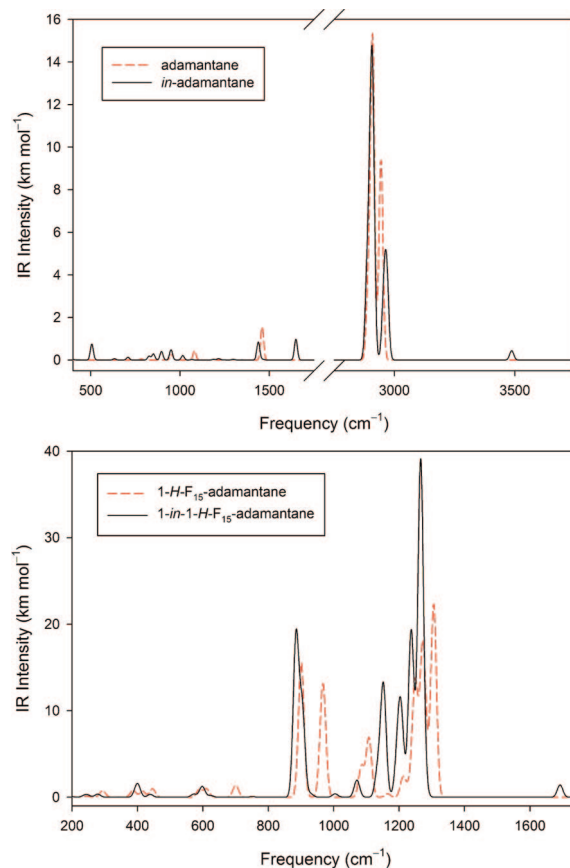
In addition to unimolecular stability, bimolecular stability is necessary for a compound to be isolable in macroscopic quantities. Reactivity of **1** with water, oxygen, and a second molecule of **1** was probed computationally by forcing molecules directly together while allowing other geometric parameters to relax. No evidence of reactivity was found below 400 kJ mol<sup>-1</sup>. Isopotential searching<sup>9</sup> also did not reveal facile bimolecular reactions.

Bimolecular reactions with still other species could hinder isolation of *in*-adamantanes but have not been investigated. For example, as suggested by a reviewer, hydride or fluoride abstraction could produce stable, nonclassical carbocations. Similar ions have been prepared by McMurry and co-workers.<sup>10</sup>

The predicted infrared spectra for **1** and **2** are compared with their conventional *out* isomers in Figure 1. The stretching frequency for the inverted C–H bond is strongly blue-shifted, to about 3490 cm<sup>-1</sup> in **1** and about 3340 cm<sup>-1</sup> in **2**. The associated CH bending frequencies are also blue-shifted, by about 300 cm<sup>-1</sup> in **1** and about 400 cm<sup>-1</sup> in **2**.

Decoupled <sup>1</sup>H and <sup>13</sup>C NMR spectra were computed, with shifts relative to tetramethylsilane. The values for the inverted methine group of **1** are distinctive: 7.5 ppm for <sup>1</sup>H and 21 ppm for <sup>13</sup>C. The shifts for **2** are less unusual: 3.0 ppm for <sup>1</sup>H and 42 ppm for <sup>13</sup>C. To gauge the reliability of the computations, experimental<sup>11</sup> methine shifts for *out*-adamantane of 1.88 ppm and 28.43 ppm for <sup>1</sup>H and <sup>13</sup>C may be compared with computed values of 1.9 and 33 ppm.

The inverted C–H bonds in **1** and **2** (102.5 and 103.9 pm, respectively) are compressed relative to the corresponding *out*-

**FIGURE 1.** Comparison of IR spectra of isomers.

isomers (109.9 and 109.6 pm), consistent with their higher stretching frequencies. Distances from the inverted H-atom to the nonbonded C-atoms in **1** are 170.3 (tertiary), 177.4 ( $\alpha$ ), and 191.8 pm ( $\gamma$ ). In **2**, those distances are slightly shorter: 169.6, 177.3, and 190.1 pm, respectively. The inverted HCC bond angle is acute, 82.3° in **1** and 83.8° in **2**. Thus, the inverted carbon has all four covalent bonds lying within one hemisphere, as in many propellanes.<sup>12</sup> The inverted bridgehead is only slightly pyramidal; the sum of its three CCC bond angles is 354.7° in **1** and 356.6° in **2**, as compared with 328.1° in *out*-adamantane and 328.2° in *out*-1-*H*-F<sub>15</sub>-adamantane. There is some compensation by the other bridgeheads; their angle sums are 323.9° in **1** and 323.3° in **2**. For comparison, the corresponding bridgehead angle sums for some propellanes are 284.5°, 360.0°, and 359.8° for [1.1.1]propellane, [2.2.2]propellane, and 1,3-didehydroadamantane, respectively (present calculations).

Although many larger *in*-molecules have been prepared, all have normal tetrahedral coordination at the formally inverted bridgehead.<sup>7</sup> Endohedral hydrogenation has been proposed previously for fullerenes<sup>13</sup> and a related structure has been calculated for a high-energy isomer of the endohedral dodecahedrane complex H@C<sub>20</sub>H<sub>20</sub>.<sup>14</sup>

Strained molecules such as **1** and **2**, possessing an inverted bridgehead, are predicted to be isolable in macroscopic quantities. Experimental verification (or refutation) presents a novel synthetic challenge.

(6) Certain commercial materials and equipment are identified in this paper in order to specify procedures completely. In no case does such identification imply recommendation or endorsement by the National Institute of Standards and Technology, nor does it imply that the material or equipment identified is necessarily the best available for the purpose.

(7) Alder, R. W.; East, S. P. *Chem. Rev.* **1996**, *96*, 2097–2111.

(8) Zachariah, M. R.; Westmoreland, P. R.; Burgess, D. R., Jr.; Tsang, W.; Melius, C. F. *J. Phys. Chem.* **1996**, *100*, 8737–8747.

(9) Irikura, K. K.; Johnson, R. D., III. *J. Phys. Chem. A* **2000**, *104*, 2191–2194.

(10) McMurry, J. E.; Lectka, T. *J. Am. Chem. Soc.* **1993**, *115*, 10167–10173.

(11) Pouchert, C. J.; Behnke, J. *The Aldrich Library of 13C and 1H FT NMR Spectra*, 1st ed.; Aldrich Chemical Co.: Milwaukee, WI, 1993.

(12) Wiberg, K. B. *Acc. Chem. Res.* **1984**, *17*, 379–386.

(13) Saunders, M. *Science* **1991**, *253*, 330–331.

(14) Moran, D.; Stahl, F.; Jemmis, E. D.; Schaefer, H. F., III; Schleyer, P. v. R. *J. Phys. Chem. A* **2002**, *106*, 5144–5154.

### Computational Details

Isopotential searches were performed on PM3 and HF/3-21G energy surfaces. Traditional exploratory calculations were done at the B3LYP/6-31G(d) level. MP2/6-31G(d) was used for final geometry optimizations and vibrational spectra. Core electrons were uncorrelated in all post-HF calculations. Harmonic vibrational frequencies were scaled by 0.9421 for fundamentals<sup>15</sup> and by 0.9670 for zero-point energies<sup>16</sup> and were unscaled for computing thermodynamic partition functions. CCSD(T)/aug-cc-pVTZ energies could not be computed with the available resources, so they were estimated as  $E[\text{CCSD(T)/6-31G(d)}] + E[\text{MP2/aug-cc-pVTZ}] - E[\text{MP2/6-31G(d)}]$ . To keep the number of basis functions consistent between isomers when using the aug-cc-pVTZ basis sets, no deletions were allowed for near-linear dependencies. A Gaussian

line shape of width  $20 \text{ cm}^{-1}$  was used for preparing Figure 1. The reaction mediated by each transition structure was confirmed by intrinsic reaction coordinate calculations.<sup>17</sup> Unimolecular half-lives were computed using transition-state theory with the Wigner tunneling correction; imaginary transition frequencies were not scaled. Vertical excitation energies were computed using time-dependent B3LYP/6-311++G(d,p). NMR spectra were computed using GIAO-MP2/6-311+G(2d,p).

**Supporting Information Available:** Atomic coordinates, selected internal coordinates, energies, vibrational data, <sup>1</sup>H and <sup>13</sup>C NMR shifts, and ideal-gas thermodynamic functions. This material is available free of charge via the Internet at <http://pubs.acs.org>.

JO801806W

(15) Irikura, K. K.; Johnson, R. D., III; Kacker, R. N. *J. Phys. Chem. A* **2005**, *109*, 8430–8437.

(16) Scott, A. P.; Radom, L. *J. Phys. Chem.* **1996**, *100*, 16502–16513.

(17) Gonzalez, C.; Schlegel, H. B. *J. Chem. Phys.* **1989**, *90*, 2154–2161.